Langmuir

Article

pubs.acs.org/Langmuir

Revisiting the Fine Structure of the Triple Line

E. Bormashenko,*[,†,‡] A. Musin,[†,‡] G. Whyman,[†] Z. Barkay,[§] and M. Zinigrad[‡]

[†]Department of Physics, and [‡]Department of Chemical Engineering and Biotechnology, Ariel University, Post Office Box 3, Ariel 40700, Israel

[§]Wolfson Applied Materials Research Center, Tel Aviv University, Ramat-Aviv 69978, Israel

ABSTRACT: The fine structure of the triple line for water droplets deposited on porous polymer substrates was investigated. Substrates were obtained with the breath-figures self-assembly. Water droplets demonstrated the pronounced Cassie−Baxter wetting regime. The triple line was imaged with environmental scanning electron microscopy. The roughness of a triple line was characterized with its averaged root-mean-square (rms) width $w(L)$, and its scaling experimental dependence upon the length L of the triple line $w(L) \propto L^{\zeta}$ was analyzed. The values of exponents in the range of 0.60−063 were established. The deduced values of ζ evidence the local nature of the triple-line elasticity and support the idea that the elastic potential of the triple line includes only even powers of the displacement.

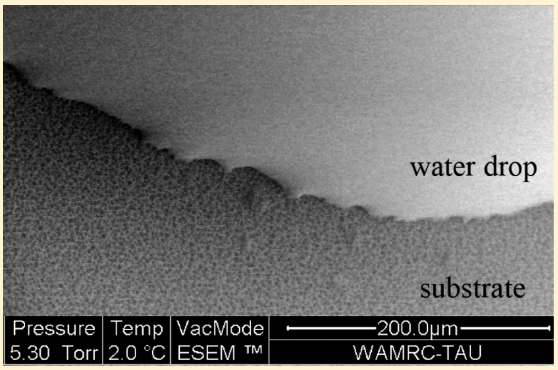

INTRODUCTION

Wetting phenomena play a major role in numerous natural and technological endeavors, including climate and soil science, plant biology and biophysics, manufacturing of films and fibers, etc.[1−4] When liquid wets a solid substrate (a solid surface may be flat or rough, homogeneous or heterogeneous), two main static scenarios are possible: the liquid spreads completely to lower the surface energy of interfaces or it forms a "cap" with the apparent contact angle θ (Figure 1). The latter case is known as partial

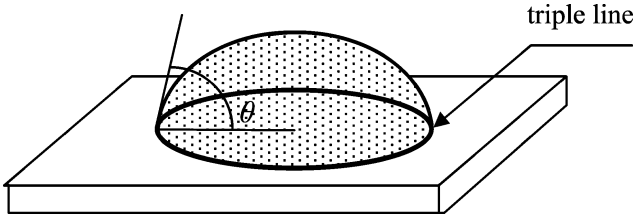

Figure 1. Drop resting on a substrate with a contact angle θ.

wetting. The line at which solid, liquid, and gaseous phases meet is called the triple (or three-phase) line (TL).[1,5] The natural macroscopic parameter characterizing wetting is the apparent contact angle. Regrettably, the contact angle is not unique even for the ideal solid surface/liquid pair, because of the phenomenon of the contact angle hysteresis.[6−11]

It is well-accepted that the peculiarities of the wetting regime are governed to a great extent by the wetting situation occurring in the nearest vicinity of the TL.[12−15] Hence, the area adjacent to the TL has been studied intensively by various experimental methods, including optical and environmental scanning electron microscopies.[16−20] It was established that the TL possesses a complicated fine structure depending upon the kind and density of heterogeneities appearing on the solid surface.[16−22] The TL is anchored and distorted by the heterogeneities. This "pinning" of the TL is one of the sources of the hysteresis of the contact angle.[5,13,23,24] De Gennes and Joanny suggested[25,26] that the magnitude of the distortion of the TL is controlled by the balance between the pinning potential and the elastic energy of the line. According to de Gennes and Joanny,[25,26] the elastic energy of the TL is nonlocal (a local deformation of the TL depends upon deformations of its remote parts), because deformations of the line are accompanied by distortions of the liquid/vapor interface.

Scaling laws describing the shape of the TL are of particular interest, and they were studied earlier.[16−18] A systematic study of the fine structure of the TL was started by Decker and Garoff.[16] They investigated water droplets placed on a fluoro polymer, degraded by ultraviolet (UV), and they stated that the characteristic wavelength of the distorted TL was much larger than the characteristic dimensions of "spots" produced by UV. The results reported by Decker and Garoff were discussed by de Gennes et al., who supposed that the irradiated areas may be spatially correlated. On the other hand, in their more recent research,[27] Moulinet and co-workers developed a statistical approach to the analysis of the dependence of the TL fine structure upon chaotic chromium defects. They came to the conclusion that the elastic potential of the TL is of a local nature. Some researchers[28] pointed to the anharmonicity of the elastic potential of the TL. It should be mentioned that the experimental data related to the scaling laws governing the distortion of the TL are scarce and contradictory, and the problem calls for further research.

Our work is devoted to the fine structure of the TL observed for droplets placed on honeycomb reliefs manufactured with the

Received: August 9, 2013
Revised: October 21, 2013
Published: October 21, 2013

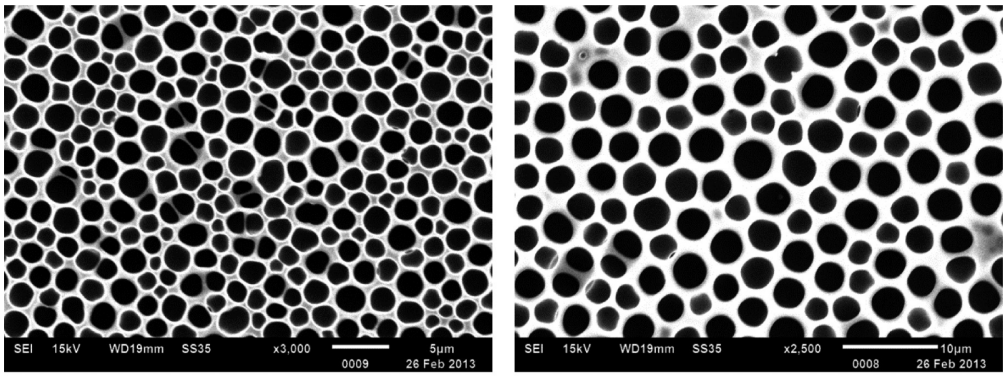

a b

Figure 2. SEM images of samples: (a) sample 1 (scale bar is 5 μm) and (b) sample 2 (scale bar is 10 μm).

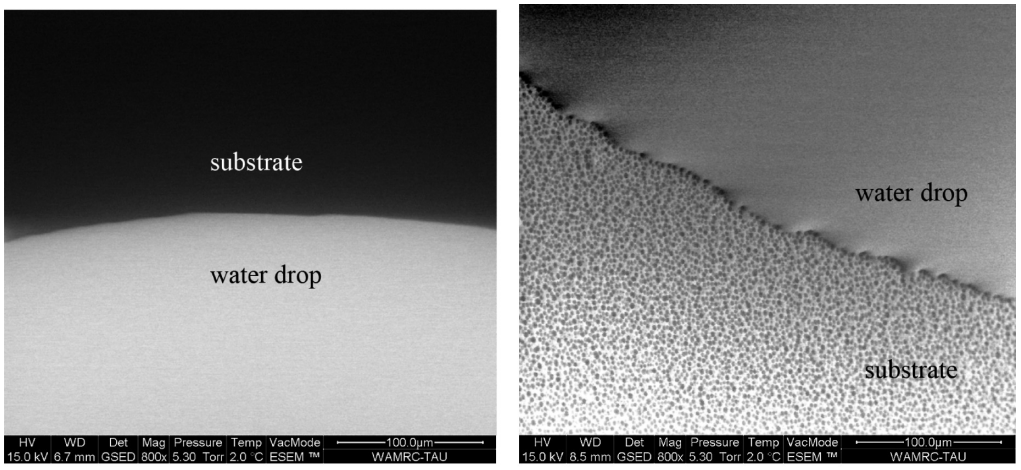

a b

Figure 3. ESEM images of the TL on a (a) smooth and (b) heterogeneous PC surface.

breath-figures self-assembly.[29−33] The fine structure of the TL was studied with the environmental scanning electron microscopy (ESEM), supplying an effective tool for studying wetting phenomena.[19,34] Our paper keeps a macroscopic approach and neglects the impact of van der Waals forces, which may also be essential for constituting the shape of the TL.[1,2,5,35,36]

EXPERIMENTAL SECTION

Substrates. Heterogeneous surfaces prepared with the dip-coating method described earlier[37] comprised a porous polycarbonate (PC) self-assembled layer with the thickness of about 2 μm, deposited on a polypropylene (PP) substrate of 30 μm thickness. The average diameter of pores calculated with scanning electron microscopy (SEM) images was 1.83 ± 0.03 μm on sample 1 and 2.83 ± 0.03 μm on sample 2 (Figure 2). Pores with an average area of about 2.6 μm^2 (sample 1) and 6.3 μm^2 (sample 2) covered about 40 and 35% of the surfaces, respectively. The atomically flat PC films, obtained by pouring PC solutions on water,[33] demonstrated "as placed" contacted angles of 81.8° ± 0.3° (Rame-Hart goniometer model 500-F1, with precision of 0.1°). This value is close to the value of the equilibrium (Young) contact angle.[38] The apparent contact angles established on porous PC reliefs were 114.4° ± 0.2° (sample 1) and 103.2° ± 0.3° (sample 2). It is seen that the Young contact angle inherent to the flat PC is acute, whereas the apparent contact angle on the rough surface is obtuse. Therefore, it is reasonable to suggest that the Cassie wetting regime occurs.[1,2,5,33] Thus, the droplet in our case is partially supported by polymer (PC) and partially supported by air cushions.

Imaging of the TL. Images of TLs were taken with ESEM at magnifications varying from 800× to 4000×. Water droplets of 10 μL in volume were placed on a substrate (samples 5 × 5 mm^2) in the ESEM chamber at the relative humidity of 100% under a temperature of 2 °C and pressure of 5.3 Torr. Further pressure variation from 5.3 to 1.4 Torr was used for investigation of TL motion. The substrate might be tilted to a few degrees angle for better visualization of the TL. Snapshots of the TL were taken both in static position and during its motion with the rate of 1 frame/2 s. Typical ESEM images are depicted in Figure 3.

The diameter of droplets was about 2 mm; therefore, the sections of TL with a length of up to 200 μm (which is much more than the short-range correlation length) may be considered as linear segments. The position of TL was located on ESEM images using the Engauge Digitizer 4.1 free software and characterized by the linear coordinates x along a TL and y in the perpendicular direction (direction of actual or possible motion) (Figure 4). The main source of inaccuracy in locating the TL position was the image resolution itself, i.e., 0.3 μm/pixel for 800× magnification. Taking this into account, we could locate points on a path with the interval of Δx = 0.6 μm with reliable accuracy.

RESULTS AND DISCUSSION

Range Order of the Reliefs. It was shown earlier,[39] by calculating the autocorrelation functions, that, even for the most ordered breath-figures patterns prepared with the described dip-coating method,[37] the centers of holes with a mean diameter of about 2 μm are spatially correlated only on a short-range order, with a correlation length of about 5 μm, with no long-range order. As well, the order range can be evaluated quantitatively by

dx.doi.org/10.1021/la403086w | Langmuir 2013, 29, 14163−14167

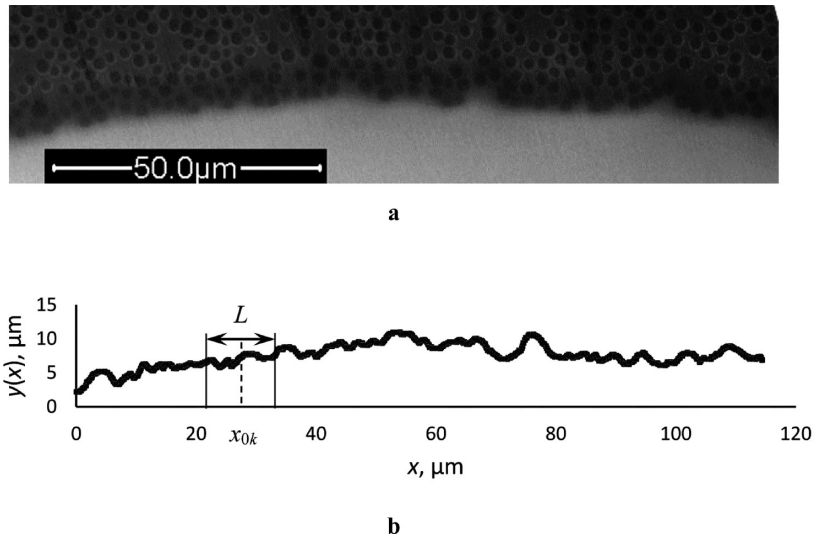

Figure 4. (a) ESEM image of TL and (b) its graphical representation.

calculation of the conformational entropy based on Voronoi polygons.[40] According to this method, the entropy S of the pattern is calculated with the formula $S = -\sum_n P_n \ln P_n$, where P_n is the fraction of polygons having the coordination number n. Analysis of packing by constructing the Voronoi polygons yielded the values of conformational entropy $S = 1.24$ for sample 1 and $S = 1.08$ for sample 2. These values are markedly less than the value of 1.71 reported for a case of fully random distribution[40] but much more than the values of 0.41−0.48 calculated for a uniform distribution[41] of pores on surfaces with breath-figure patterns very similar to our samples in the packing density and dimensions of pores. Finally, comparing the surface tension of the water−PC interface γ_{SL} (which is about 40 mJ/m^2) to that of the water−air interface ($\gamma = 72$ mJ/m^2), we can characterize our samples as having strong, dense partially ordered, circular defects possessing a short-range order.

Fourier Expansion of the Path. Characteristic structural elements, which determine the roughness of the TL, can be revealed using a corresponding Fourier expansion of the TL shape.

$$y(x) = \sum_n a_n \, e^{iq_n x} \qquad q_n = 2\pi/\lambda_n \tag{1}$$

The modules of typical values of the expansion coefficients a_n corresponding to wavelengths λ_n are presented in Figure 5. As seen, the dominant contributions to $y(x)$ are due to wavelengths of about 50−80 μm. Therefore, the main factor governing the roughness of the TL is related to the irregularity of the distribution of the defects and not the defects themselves, which are on the order of a few micrometers. Thus, a distinct hierarchy of characteristic lengths appears: the dominate wavelengths in the Fourier expansion of the TL is about 50−80 μm, which is much larger than a correlation length of pores (~5 μm), which is, in turn, larger but comparable to the average diameter of pores (~2 μm). All of these characteristic lengths are much less than the diameter of a droplet, which is of 1 mm.

Motion of the TL. The motion of the TL was stimulated by decreasing pressure in the chamber. The velocity of TL motion was less than 5 μm/s, which characterized the motion as quasi-static, and roughness of the TL did not depend upon velocity.[18] The chamber was evacuated quickly to the working pressure of 5.4 Torr. The further slow decrease in the pressure accompanied

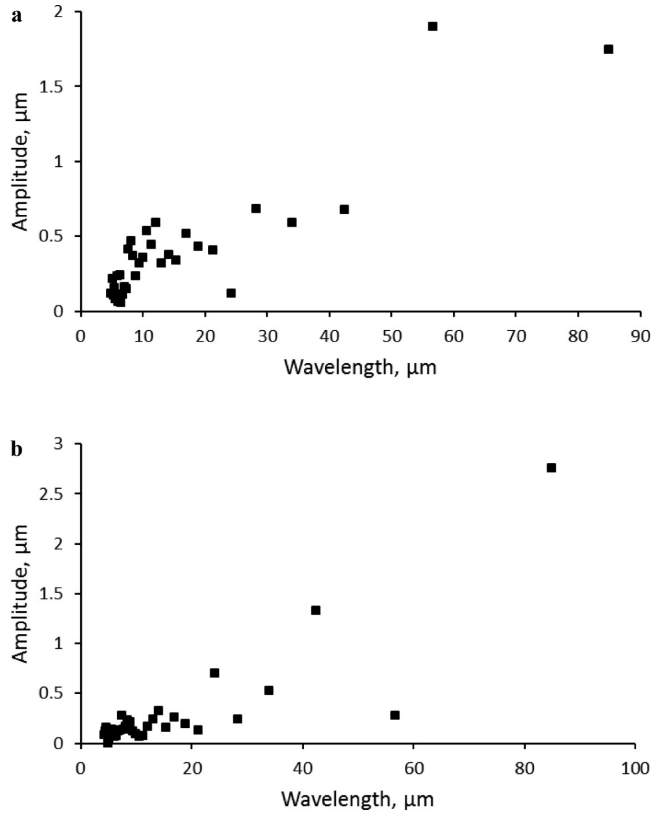

Figure 5. Typical Fourier spectra of the TL shape on (a) sample 1 and (b) sample 2.

by evaporation of the droplet surprisingly led to the TL expansion outward from the droplet. Then, the TL stopped and afterward, moved backward, and the droplet collapsed. This may be explained by the Kelvin effect, expressed with the formula

$$\ln \frac{p}{p_0} = \frac{2\gamma V_m}{rRT} \tag{2}$$

where p and p_0 are the vapor and saturated vapor pressures, correspondingly, γ is the surface tension, V_m is the molar volume of water, R is the universal gas constant, T is the temperature, and

dx.doi.org/10.1021/la403086w | Langmuir 2013, 29, 14163−14167

r is the curvature radius of a droplet (the radius of a spherical cap). According to eq 2, the decrease in pressure p in the chamber at a constant temperature leads to the increase in the curvature radius r, which means expansion of the TL. Indeed, under conservation of the contact angle θ, the contact radius $r \sin \theta$ grows with r. Competing evaporation accompanied with the mass loss leads to the eventual collapse of the droplet.

Calculation of the Roughness of the TL. The roughness of the TL as a whole is usually characterized by its averaged root-mean-square (rms) width $w(L)$ dependent upon its length L. The main part of discussion in the literature is devoted to the value of the exponent in the scaling relation[1,16−18,27−28]

$$w(L) \propto L^{\zeta} \tag{3}$$

A TL with a total length D was presented as N points (x_i, y_i) separated by the span Δx. It may be divided into segments with length $l < L < D/2$ centered at $n(L)$ points x_{0k} ($l \sim 5$ μm is the correlation length mentioned above). The mean position $\overline{y}(L,x_{0k})$ (see Figure 4b), rms width $\sigma(L,x_{0k})$, and its average $w(L)$ on ensemble of segments with the same L were calculated according to the formulas:

$$\overline{y}(L, x_{0k}) = \frac{1}{L}\sum_{i=1}^{n(L)} y_i \Delta x = \frac{\Delta x}{L}\sum_{i=1}^{n(L)} y_i = \frac{1}{n(L)}\sum_{i=1}^{n(L)} y_i \tag{4}$$

$$\sigma^2(L, x_{0k}) = \frac{1}{L}\sum_{i=1}^{n(L)} [y_i - \overline{y}(L, x_{0k})]^2 \Delta x = \frac{1}{n(L)}\sum_{i=1}^{n(L)} [y_i - \overline{y}(L, x_{0k})]^2 \tag{5}$$

$$w(L) = \left(\frac{1}{D-L}\sum_{k} \sigma^2(L, x_{0k})\Delta x_{0k}\right)^{0.5} \tag{6}$$

Equation 6 means averaging on the ensemble of segments of L length, with x_{0k} being the center coordinate of the kth segment, and Δx_{0k} is the distance between the centers.

The typical dependences of w upon L are presented in Figure 6 (here, the TL is expanding with an average velocity of 1.4 μm/s).

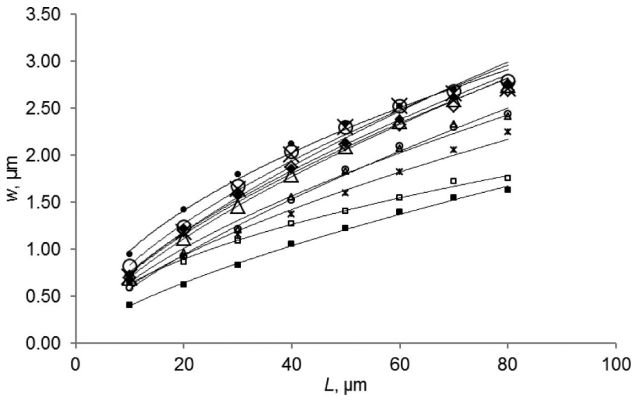

Figure 6. Average roughness w of the TL versus length L. Different curves present dependences $w(L)$ for consequent positions of the TL during its expansion.

It is seen that most of the curves are almost parallel. The shift is explained by the movement of the TL in a fixed coordinate system. If each curve were shifted by its own average y, the points on the graph would almost coincide. Taking into account only dependences with the correlation coefficient $R^2 > 0.99$, we obtained $\zeta = 0.63 \pm 0.02$. The results of the calculation performed for the receding line look very similar to Figure 6 and give $\zeta = 0.60 \pm 0.05$; therefore, the roughness exponent in eq 3 may be evaluated as $\zeta = 0.62$. The error introduced into these estimations by image processing is evaluated as 0.01.

The values of ζ are close for the extension and retreat of the TL. This means that the elastic potential of the TL may contain only the even powers of the TL deformation, because under retreat, the deformation changes its overall sign. Indeed, as it was shown[28] in the work of Rosso and Krauth, the anharmonic elastic potential of the TL, containing the second and fourth powers of the TL displacement, leads to almost the same value of ζ equal to 0.63. On the other hand, the same values of ζ for both directions of the TL movement support the presence of the Cassie wetting state with air trapped under a droplet, as mentioned in the Experimental Section.

The classical model proposed by Joanny and de Gennes assumed a pronounced nonlocal behavior of the TL, when the local deformation of the TL depends upon the deformation of its remote parts.[26] For nonlocal models, the one-loop calculations supplied a roughness exponent equal to $^1/_3$, which at the time was believed to be exact.[42,43] The mathematical simulations based on the more comprehensive nonlocal models gave rise to the values of ζ in the range of 0.34−0.39.[43] Experiments performed with helium-4 deposited on a strongly disordered cesium substrate supplied the roughness exponent $\zeta = 0.56 \pm 0.03$.[44] The values of ζ = 0.6−0.63 established in our paper coincide with the roughness exponents obtained for the crack propagation fronts in plastics[45,46] and interface roughening in porous media.[47] Kardar noted that a value of ζ = 0.63 appears in a number of different models based on directed percolation.[48] In these models, the mobile interface is stopped by a direct percolation cluster of pinning sites.[48] This suggestion corresponds to the experimental situation occurring in our research, if we suppose that the TL is pinned by a cluster of short-ordered pores, as discussed in the beginning of this section.

CONCLUSION

The fine structure of the TL in the situation of the Cassie wetting, when a water droplet was deposited on the porous polymer (polycarbonate) substrate, was studied. The porous substrate was obtained with the "breath-figures" self-assembly and demonstrated short-range ordering on a scale of several micrometers.

The roughness of a TL was characterized with its averaged rms width $w(L)$, and the dependence upon the scaling length L of the TL $w(L) \propto L^{\zeta}$ was analyzed. The obtained value of the exponent ζ evidence the local nature of the TL elasticity, at least in the considered case of strong defects partly ordered on a micrometrical scale.

The close values of the exponents obtained in the present work in the cases of the retreating (0.60 ± 0.05) and expanding (0.63 ± 0.02) TL indicate that the elastic potential of the TL contains only even powers of the displacement. These values of roughness exponents were also observed for crack propagation fronts in plastics and interface roughening in porous media. This coincidence hints at the universal character of ζ = 0.6−0.63 appearing in models based on direct percolation.

AUTHOR INFORMATION

Corresponding Author

*E-mail: edward@ariel.ac.il.

Notes

The authors declare no competing financial interest.

■ ACKNOWLEDGMENTS

Albina Musin is grateful for the support of the Milken Family Foundation for her fellowship.

■ REFERENCES

(1) de Gennes, P. G.; Brochard-Wyart, F.; Quéré, D. *Capillarity and Wetting Phenomena*; Springer: Berlin, Germany, 2003.
(2) Erbil, H. Y. *Surface Chemistry of Solid and Liquid Interfaces*; Blackwell: Oxford, U.K., 2006.
(3) Starov, V. M.; Velarde, M. G.; Radke, Cl. J. *Wetting and Spreading Dynamics*; CRC Press: Boca Raton, FL, 2007; Surfactant Science Series, Vol. *138*.
(4) Adamson, A. W.; Gast, A. P. *Physical Chemistry of Surfaces*, 6th ed.; Wiley-Interscience Publishers: New York, 1990.
(5) Bormashenko, E. *Wetting of Real Surfaces*; De Gruyter: Berlin, Germany, 2013.
(6) Marmur, A. A guide to the equilibrium contact angles maze. In *Contact Angle Wettability and Adhesion*; Mittal, K. L., Ed.; Brill/VSP: Leiden, Netherlands, 2009; Vol. *6*, pp 3−18.
(7) Extrand, C. W.; Kumagai, Y. An experimental study of contact angle hysteresis. *J. Colloid Interface Sci.* **1997**, *191*, 378−383.
(8) Starov, V. Static contact angle hysteresis on smooth, homogeneous solid substrates. *Colloid Polym. Sci.* **2013**, *291*, 261−270.
(9) Bormashenko, E. Wetting of real solid surfaces: New glance on well-known problems. *Colloid Polym. Sci.* **2013**, *291*, 339−342.
(10) Priest, C.; Sedev, R.; Ralston, J. A quantitative experimental study of wetting hysteresis on discrete and continuous chemical heterogeneities. *Colloid Polym. Sci.* **2013**, *291*, 271−277.
(11) Quéré, D. Wetting and roughness. *Annu. Rev. Mater. Res.* **2008**, *38*, 71−99.
(12) Shanahan, M. E. R. Simple theory of "stick-slip" wetting hysteresis. *Langmuir* **1995**, *11*, 1041−1043.
(13) Yaminsky, V. V. Hydrophobic transitions. In *Apparent and Microscopic Contact Angles*; Drelich, J., Laskowski, J. S., Mittal, K. L., Eds.; VSP: Utrecht, Netherlands, 2000, pp 47−93.
(14) Gao, L.; McCarthy, Th. J. How Wenzel and Cassie were wrong. *Langmuir* **2007**, *23*, 3762−3765.
(15) Nosonovsky, M. On the range of applicability of the Wenzel and Cassie equations. *Langmuir* **2007**, *23*, 9919−9920.
(16) Decker, E. L.; Garoff, S. Contact line structure and dynamics on surfaces with contact angle hysteresis. *Langmuir* **1997**, *13*, 6321−6332.
(17) Rolley, E.; Guthmann, C.; Gombrowicz, R.; Repain, V. Roughness of the contact line on a disordered substrate. *Phys. Rev. Lett.* **1998**, *80*, 2865−2868.
(18) Moulinet, S.; Rosso, Al.; Krauth, W.; Rolley, E. Width distribution of contact lines on a disordered substrate. *Phys. Rev. E: Stat., Nonlinear, Soft Matter Phys.* **2004**, *69*, 035103.
(19) Bormashenko, Ed.; Bormashenko, Ye.; Stein, T.; Whyman, G.; Pogreb, R. Environmental scanning electron microscopy study of the fine structure of the triple line and Cassie−Wenzel wetting transition for sessile drops deposited on rough polymer substrates. *Langmuir* **2007**, *23*, 4378−4382.
(20) Leh, A.; N'guessan, H. E.; Fan, J.; Bahadu, Pr.; Tadmor, R.; Zhao, Y. On the role of the three-phase contact line in surface deformation. *Langmuir* **2012**, *28*, 5795−5801.
(21) Bormashenko, E. Why does the Cassie−Baxter equation apply? *Colloids Surf., A* **2008**, *324*, 47−50.
(22) Saiz, E.; Tomsia, A. P.; Cannon, R. M. Ridging effects on wetting and spreading of liquids on solids. *Acta Mater.* **1998**, *46*, 2349−2361.
(23) Li, D.; Neumann, A. W. Surface heterogeneity and contact angle hysteresis. *Colloid Polym. Sci.* **1992**, *270*, 498−504.
(24) Bormashenko, E.; Musin, A.; Zinigrad, M. Evaporation of droplets on strongly and weakly pinning surfaces and dynamics of the triple line. *Colloids Surf., A* **2011**, *385*, 235−240.
(25) de Gennes, P. G. Wetting: Statics and dynamics. *Rev. Mod. Phys.* **1985**, *57*, 827−863.
(26) Joanny, J. F.; de Gennes, P. G. A model for contact angle hysteresis. *J. Chem. Phys.* **1984**, *81*, 552−562.
(27) Moulinet, S.; Guthmann, C.; Rolley, E. Roughness and dynamics of a contact line of a viscous fluid on a disordered substrate. *Eur. Phys. J. E: Soft Matter Biol. Phys.* **2002**, *8*, 437−443.
(28) Rosso, A.; Krauth, W. Origin of the roughness exponent in elastic strings at the depinning threshold. *Phys. Rev. Lett.* **2001**, *87*, 187002-1−187002-4.
(29) Widawski, G.; Rawiso, B.; Francois, B. Self-organized honeycomb morphology of star-polymer polystyrene films. *Nature* **1994**, *369*, 387−389.
(30) Srinivasarao, M.; Collings, D.; Philips, A.; Patel, S. Three-dimensionally ordered array of air bubbles in a polymer film. *Science* **2001**, *292*, 79−83.
(31) Xue, L.; Zhang, J.; Han, Y. Phase separation induced ordered patterns in thin polymer blend films. *Prog. Polym. Sci.* **2012**, *37*, 564−594.
(32) Hernández-Guerrero, M.; Stenzel, M. H. Honeycomb structured polymer films via breath figures. *Polym. Chem.* **2012**, *3*, 563−577.
(33) Bormashenko, E.; Balter, S.; Aurbach, D. On the nature of the breath figures self-assembly in evaporated polymer solutions: Revisiting physical factors governing the patterning. *Macromol. Chem. Phys.* **2012**, *213*, 1742−1747.
(34) Barkay, Z. Dynamic study of nanodroplet nucleation and growth on self-supported nanothick liquid films. *Langmuir* **2010**, *26*, 18581−18584.
(35) Starov, V. M.; Velarde, M. G. Surface forces and wetting phenomena. *J. Phys: Condens. Matter* **2009**, *21*, 464121.
(36) Ruckenstein, E.; Berim, G. O. Microscopic description of a drop on a solid surface. *Adv. Colloid Interface Sci.* **2010**, *157*, 1−33.
(37) Bormashenko, E.; Pogreb, R.; Stanevsky, O.; Bormashenko, Ye.; Stein, T.; Gaisin, V.-Z.; Cohen, R.; Gengelman, O. Mesoscopic patterning in thin polymer films formed under the fast dip-coating process. *Macromol. Mater. Eng.* **2005**, *290*, 114−121.
(38) Tadmor, R.; Yadav, Pr. S. As-placed contact angles for sessile drops. *J. Colloid Interface Sci.* **2008**, *317*, 241−246.
(39) Bormashenko, E.; Malkin, A.; Musin, A.; Bormashenko, Ye.; Whyman, G.; Litvak, N.; Barkay, Z.; Machavariani, V. Mesoscopic patterning in evaporated polymer solutions: Poly(ethylene glycol) and room-temperature-vulcanized polyorganosilanes/siloxanes promote formation of honeycomb structures. *Macromol. Chem. Phys.* **2008**, *209*, 567−576.
(40) Limaye, A. V.; Narhe, R. D.; Dhote, A. M.; Ogale, S. B. Evidence for convective effects in breath figure formation on volatile fluid surfaces. *Phys. Rev. Lett.* **1995**, *76*, 3762−3765.
(41) Park, M. S.; Kim, J. K. Breath figure patterns prepared by spin coating in a dry dnvironment. *Langmuir* **2004**, *20*, 5347−5352.
(42) Narayan, O.; Fisher, D. S. Threshold critical dynamics of driven interfaces in random media. *Phys. Rev. B: Condens. Matter Mater. Phys.* **1993**, *48*, 7030−7042.
(43) Rosso, A.; Krauss, W. Roughness at the depinning threshold for a long-range elastic string. *Phys. Rev. E: Stat., Nonlinear, Soft Matter Phys.* **2002**, *65*, 025101.
(44) Prevost, A.; Rolley, E.; Guthmann, C. Dynamics of a helium-4 meniscus on a strongly disordered cesium substrate. *Phys Rev. B: Condens. Matter Mater. Phys.* **2002**, *65*, 064517.
(45) Santucci, S.; Grob, M.; Toussaint, R.; Schmittbuhl, H. A.; Maloy, K. J. Fracture roughness scaling: A case study on planar cracks. *Europhys. Lett.* **2010**, *92*, 44001.
(46) Delaplace, A.; Schmittbuhl, J.; Maloy, K. J. High resolution description of a crack front in a heterogeneous Plexiglas. *Phys. Rev. E: Stat. Phys., Plasmas, Fluids, Relat. Interdiscip. Top.* **1999**, *60*, 1337−1343.
(47) Buldyrev, S. V.; Barabasi, A.-L. Anomalous interface roughening in porous media: Experiment and model. *Phys Rev. A: At., Mol., Opt. Phys.* **1992**, *45*, R8313−R8316.
(48) Kardar, M. Nonequilibrium dynamics of interfaces and lines. *Phys. Rep.* **1998**, *301*, 85−12.